ISSN 0040-6015, Thermal Engineering, 2015, Vol. 62, No. 1, pp. 68–75. © Pleiades Publishing, Inc., 2015.

HEAT AND MASS TRANSFER AND PROPERTIES OF WORKING FLUIDS AND MATERIALS

Investigation of the Effect of Using Tube Inserts for the Intensification of Heat Transfer[1]

K. Goodarzi, S. Y. Goudarzi, and Gh. Zendehbudi

Department of Mechanical Engineering, Yasouj University, Yasouj 75918-74831, Iran

e-mail: kgoudarzi@yu.ac.ir

Abstract—In this work, heat transfer in channels containing inserts of different shapes was investigated using computational fluid dynamics (CFD) modeling techniques taking a gaslight water heater as an example. Three types of devices inserted in the water heater tube (flow swirlers) were investigated: star-shaped, coiled wire, and classic ones in the form of twisted tapes. In the present study, the RNG k–ε turbulence model is used to model the turbulent flow regime. This numerical simulation has been performed over a Reynolds number range of 5800–18500. In the studied range of Reynolds number the maximum thermal performance factor was obtained by the starry inserts with $A_{star}/A_{inlet} = 0.50$. The results have exposed that also the use of all tube inserts leads to a considerable increase in heat transfer and pressure drop over the smooth tube. In addition, the results revealed that both heat transfer rate and friction factor in the tube equipped with starry insert were significantly higher than those in the tube fitted with the coiled wire inserts and classic twisted tape.

Keywords: heat transfer, intensification, turbulent flow, tube insert, thermal performance factor

DOI: 10.1134/S004060151501005X

It has been commonly known that the performance of heat exchangers, for single-phase flows in particular, can be improved by many intensification techniques. These techniques can be classified into active and passive techniques and compound enhancement. The active techniques require additional external power such as surface vibration and fluid injection. The passive techniques do not require direct input of external power. The use of two or more techniques (passive and/or active) in conjunction constitutes compound enhancement. Some examples of passive heat transfer enhancement methods include: insertion of porous [1–4], wire coil and helical wire coil inserts [5, 6]. The twisted tape insert provides considerable increase in heat transfer rate by formation of a swirling flow and increasing the turbulence intensity close to the tube wall. Various investigations have been performed to increase heat transfer rate using this type of insert [7–19]. In accordance with the filds synergism (the combined effect) principle, the better the coordination between the coolant flow velocity and heat flux fields, the higher the convective heat transfer coefficient. In [20], exact solutions for the synergy field were obtained and calculation results are presented. In [21, 22], the synergy field is considered as an objective function. It is shown that heat transfer increases, and the pressure drop decreases with a growth of so-called synergy parameter, which characterizes the mutual influence of velocity fields and heat flow.

[1] The article is published in the original.

In the present study, the effect of twist length on the performance of classic twisted tape and coiled wire inserts and the behavior of a novel tube insert, namely starry insert in a gaslight water heater were investigated.

DESCRIPTION OF THE GASLIGHT WATER HEATER MODEL

Physical model. The studied gaslight water heater including a bent tube with 80 fins. This fins have 1 mm thickness. The bent tube has 1.376 m length, 1 mm thickness and ellipse cross section with 19 mm large diameter and 17 mm small diameter. Three different kinds of tube inserts were investigated in this study to compare the heat transfer enhancement with the corresponding plain tubes. The coiled wire insert in square cross section with 2 mm length of side. Two different pitch length of 12 and 17 mm were considered in this study. The classic twisted tape inserts have a 15 mm width and a 1 mm thickness with two pitch length as 30 and 45 mm. The starry inserts has 0.6 mm thickness and consist of a holding rod with 2 mm diameter. These inserts are used in three surface ratios A_{star}/A_{inlet} of 0.31, 0.50 and 0.58, between the starry piece and the rod with 2 cm pitch length. The geometrical configurations of these tube insert and the part of studied water heater discussed in the present work are shown in Fig. 1.

The technical data of the studied water heater and conditions of its operation are as follows:

Reynolds number	5800–18500
Working fluid	Water
Temperature at the tube inlet, °C	27
Minimal relative pressure of water at the tube inlet, kPa	20

CFD modeling. The modeled domain consisting of tube with various tube inserts is meshed into 1005543 to 3251647 tetrahedral cells depending on different layouts. These mesh layouts are obtained through the examination of different cell sizes as no further significant changes are revealed for finer cells. Figure 2 shows an example of the meshed configuration of tube and inserts. Meshed surfaces of the studied tube inserts are also shown in this figure. According to the mentioned purpose regions inside the tube and especially close to the wall of tube inserts are meshed into finer cells due to the existence of narrow regions produced by the edges of the inserts.

Commercial CFD software ANSYS CFX 13.0 (ANSYS, Inc.) is used for the numerical solutions.

GOVERNING EQUATIONS AND BOUNDARY CONDITIONS

The flow velocities and the Reynolds number are calculated from the flow rates based on the equivalent diameter. The tube equivalent diameter D_{eq} is calculated from the volume of water V required to fill a given length L of tubing as follows [23]:

$$D_{eq} = 4V/(\pi L). \quad (1)$$

Reynolds number is calculated inside tubes as:

$$\mathrm{Re} = \frac{\rho u D_{eq}}{\mu}, \quad (2)$$

where u is the average velocity of flow, ρ is the density of fluid, μ is the dynamic viscosity of fluid.

The average Nu number is calculated based on the equivalent diameter as:

$$\mathrm{Nu} = \frac{\alpha D_{eq}}{\lambda}, \quad (3)$$

where α is the internal heat transfer coefficient at the surface of the pipe and λ is thermal conductivity of liquid.

For steady, incompressible and turbulent flow, the three-dimensional equations of continuity, momentum, energy, turbulent kinetic energy, k, and the turbulent kinetic energy dissipation, ε, in the fluid region can be expressed in the tensor form as follows [24]:

$$\frac{\partial \overline{u}_i}{\partial x_i} = 0; \quad (4)$$

$$\left.\begin{aligned}
&\frac{\partial}{\partial x_i}\rho\left(\overline{u_i u_j}\right) = -\frac{\partial p}{\partial x_i} \\
&+ \frac{\partial}{\partial x_i}\left[\mu_{\mathrm{eff}}\left(\frac{\partial \overline{u}_i}{\partial x_j} + \frac{\partial \overline{u}_j}{\partial x_i}\right) - \rho\overline{u_i' u_j'}\right]; \\
&\frac{\partial}{\partial x_j}\rho c_p\left(\overline{u}_j \overline{T}\right) = \overline{u}_j \frac{\partial \overline{p}}{\partial x_j} + \overline{u'}\frac{\partial \overline{p'}}{\partial x_j} \\
&+ \frac{\partial}{\partial x_j}\left(k\frac{\partial \overline{T}}{\partial x_j} - \rho c_p \overline{u_j' T'}\right); \\
&\frac{\partial}{\partial x_i}\left(\rho \overline{u}_i k\right) = -\frac{\partial}{\partial x_i}\left(\frac{\mu_{\mathrm{eff}}}{\sigma_\varepsilon}\frac{\partial k}{\partial x_i}\right) + \rho(\mathrm{Pr} - \varepsilon); \\
&\frac{\partial}{\partial x_i}\left(\rho \overline{u}_i \varepsilon\right) = -\frac{\partial}{\partial x_i}\left(\frac{\mu_{\mathrm{eff}}}{\sigma_\varepsilon}\frac{\partial \varepsilon}{\partial x_i}\right) \\
&+ \rho\frac{\varepsilon}{k}\left[\left(c_1 + c_3\frac{\mathrm{Pr}}{\sigma}\right)\mathrm{Pr} - c_2\varepsilon\right],
\end{aligned}\right\} \quad (5)$$

where $\mu_{\mathrm{eff}} = \mu + \mu_t$; $\mu_t = \rho c_\mu \dfrac{k^2}{\varepsilon}$ is the turbulent dynamic viscosity coefficient;

$$\mathrm{Pr} = \frac{\mu_t}{\rho}\left[2\left(\frac{\partial u_i}{\partial x_i}\right) - \frac{2}{3}(\nabla u_i)^2\right];$$

c_p is the specific heat capacity, p is pressure, and T is temperature.

The calculations were carried out at the following values of the constants appearing in system (5):

$$c_\mu = 0.09; \quad c_1 = 0.15; \quad c_2 = 1.90;$$
$$c_3 = 0.25; \quad \sigma_\varepsilon = 1.15.$$

The fluid domain is between the tube wall and classic twisted tape as shown in Fig. 3, and the boundary conditions are considered as below.

At inlet, the velocity distribution is assumed to be uniform and only the axial velocity component is nonzero. Average static pressure boundary condition is adopted, and the relative pressure is set as 0 Pa at outlet. Non-slip and smooth conditions are specified on the wall and tube inserts. The outside temperature is specified for the tube wall (700 K), and wall external heat transfer coefficient 40 W/(m^2 K) whereas, adiabatic condition is applied on the tube inserts.

RESULTS AND DISCUSSION

The present heat transfer and friction factor results for a smooth tube were first validated in terms of Nusselt number and friction factor before the

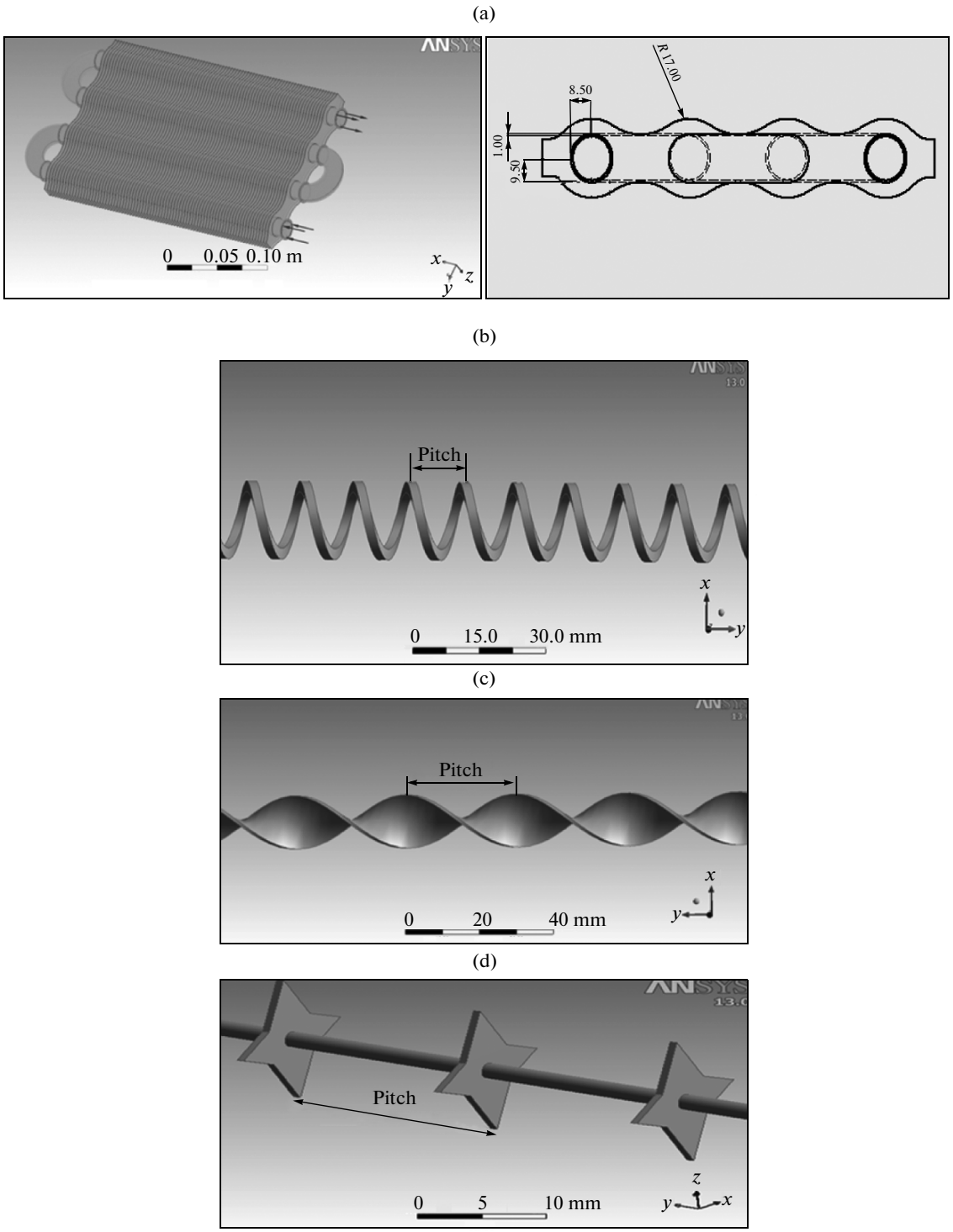

Fig. 1. The geometrical configurations of these tube inserts and the part of studied water heater. (a) Part of studied water heater; (b) the coiled wire insert; (c) classic twisted tape insert; (d) starry insert.

numerical simulations with various tubes inserts. The obtained simulations results of Nusselt number and friction factor for smooth tube were compared with the results obtained from the well-known steady state flow correlations of Gnielinski [25], Dittus and Boelter [26], Moody [27] and Petukhov [28], for the fully developed turbulent flow in tubes. Moreover, these results were compared with the experimental

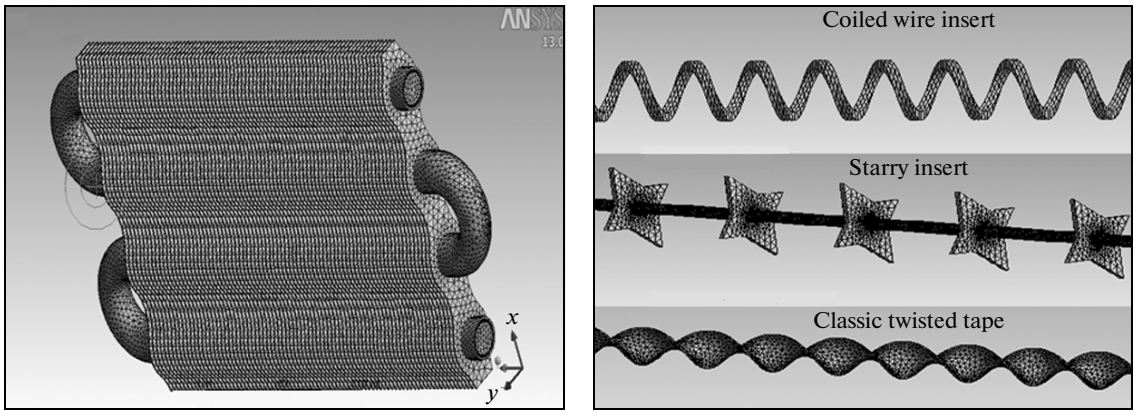

Fig. 2. The meshed configuration of tube and inserts.

results were investigated in similar conditions by S. Eiamsa-ard et al. [29].

Nusselt number correlations from Dittus and Boelter [26] is of the form:

$$\mathrm{Nu} = 0.023\,\mathrm{Re}^{0.8}\,\mathrm{Pr}^{0.4} \quad \text{for } \mathrm{Re} \geq 10^4 \tag{6}$$

Correlation from Gnielinski [25] is of the form:

$$\mathrm{Nu} = \frac{\frac{\xi}{8}(\mathrm{Re}-1000)\,\mathrm{Pr}}{1+12.7\left(\frac{\xi}{8}\right)^{0.5}\left(\mathrm{Pr}^{2/3}-1\right)} \quad \text{for } 3\times10^3 \leq \mathrm{Re} \leq 5\times10^6 \tag{7}$$

Friction factor correlations from Moody diagram [27] is of the form:

$$\xi = 0.316\,\mathrm{Re}^{-0.25} \quad \mathrm{Re} \leq 2\times10^4. \tag{8}$$

Correlation from Petukhov [28] is of the form:

$$\xi = (0.79\ln\mathrm{Re} - 1.64)^{-2} \quad \text{for } 3\times10^3 \leq \mathrm{Re} \leq 5\times10^6 \tag{9}$$

Figures 4 and 5 show comparison between the present study, the experimental results [29] and the past correlations from previous works available for steady state flow conditions in the literature for plain tube. As it can be shown in Figs. 4 and 5, the present work agrees well with the available correlations with 6.48, 6.84, 8.80 and 5.08% error percent in comparison with Gnielinski correlation, Gnielinski correlation, Dittus–Boelter and the experimental results respectively. For the Nusselt number, these errors are 7.8, 7.3 and 11.2% in comparison with Moody correlation, Petukhov correlation and the experimental results respectively.

The variations of Nusselt number with Reynolds number for the tubes fitted with various inserts are given in Fig. 6. The overall results show that the increase of the Nusselt number due to the increase of

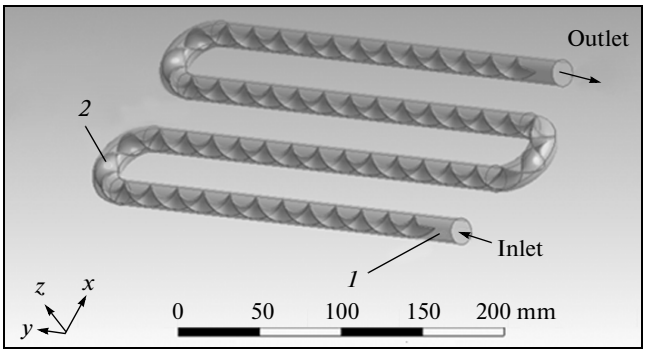

Fig. 3. The fluid domain and boundary conditions. (*1*) Fluid domain; (*2*) classic twisted tape.

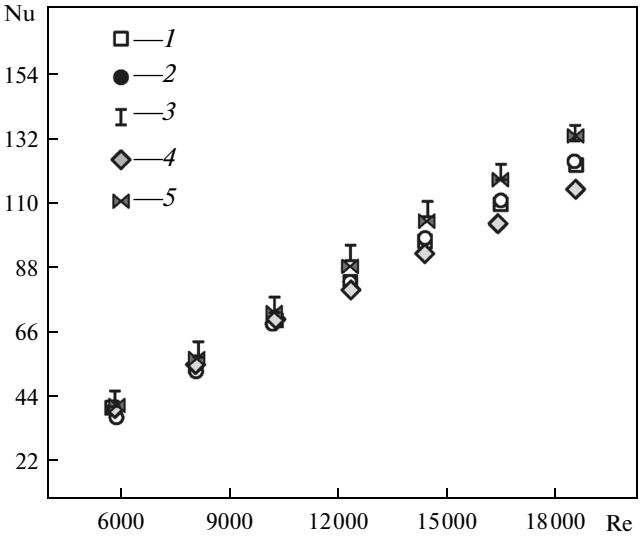

Fig. 4. Comparison between the calculated values of Nusselt number for tubes without inserts and experimental data. (*1*) Calculation according to the Gnielinski formula (the value of ξ is according to Petukhov), (*2*) calculation according to the Gnielinski formula (the value of ξ is according to Moody), (*3*) experimental data of Eiamsa-ard (2010), (*4*) experimental data of Dittus and Boelter [26], and (*5*) calculation using the CFX computer program (the present study).

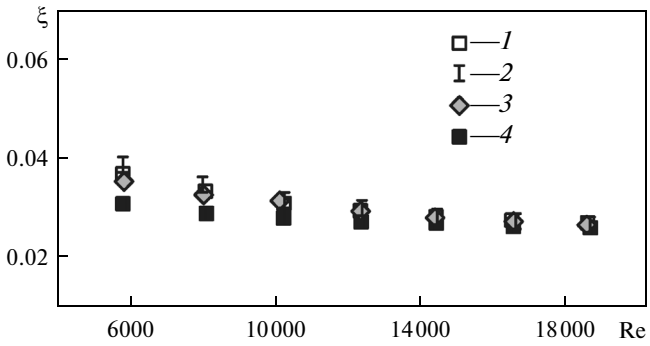

Fig. 5. Comparison between the calculated values of friction factor for the tube without inserts and experimental data. (*1*) Calculation according to the Petukhov correlation, (*2*) experimental data of Eiamsa-ard (2010), (*3*) calculation according to the Moody correlation, and (*4*) calculation according to the CFX computer program (the present study).

the Reynolds number. In addition, the result shows that in all setups when the tube is equipped with any of these inserts, the Nusselt numbers are higher than those obtained for the plain tube. This effect can be explained by a reduction in the flow cross-sectional area, an increase in turbulence intensity and an increase in tangential flow established by inserts. In Fig. 6c it can be observed that at the same Reynolds number, the use of small pitch length leads to higher Nusselt number than that of larger pitch length for both The coiled wire inserts and classic inserts. This implies that the heat transfer rate increases with decreasing tape pitch length, this trend is found to be true for both the coiled wire inserts and classic inserts. Justified by the data trend, it can be inferred that the smaller pitch length can induces the stronger swirl flow leading to thinner boundary layers along the tube wall. Consequently, heat can be transferred more efficiently over the thinner boundary layer. Moreover, the resident time of the flow increases with the smaller twist ratio due to longer flow path. Thus, the working fluid has long time for exchanging heat between the core and the wall regions. As can be seen in Fig. 6d, the use of larger surface ratios leads to higher Nusselt number than that of smaller surface ratios for the tube fitted with a starry inserts. This result may be explained by the generation of stronger turbulence intensity and more rapid mixing of flow created by this insert. In addition, the Nusselt number values of the starry inserts with $A_{star}/A_{inlet} = 0.50$ and $A_{star}/A_{inlet} = 0.58$ show small differences in the studied range of Reynolds. Figure 6 shows the Nusselt number ratio, Nu/Nu_0, which is defined as the ratio of augmented Nusselt number to Nusselt number of plain tube plotted against the Reynolds number value. As it can be shown in this figure it is obvious that the inserts' role in increasing turbulence intensity in lower velocities is more significant than in conditions in which the fluid regime is turbulent, even without embodied insert.

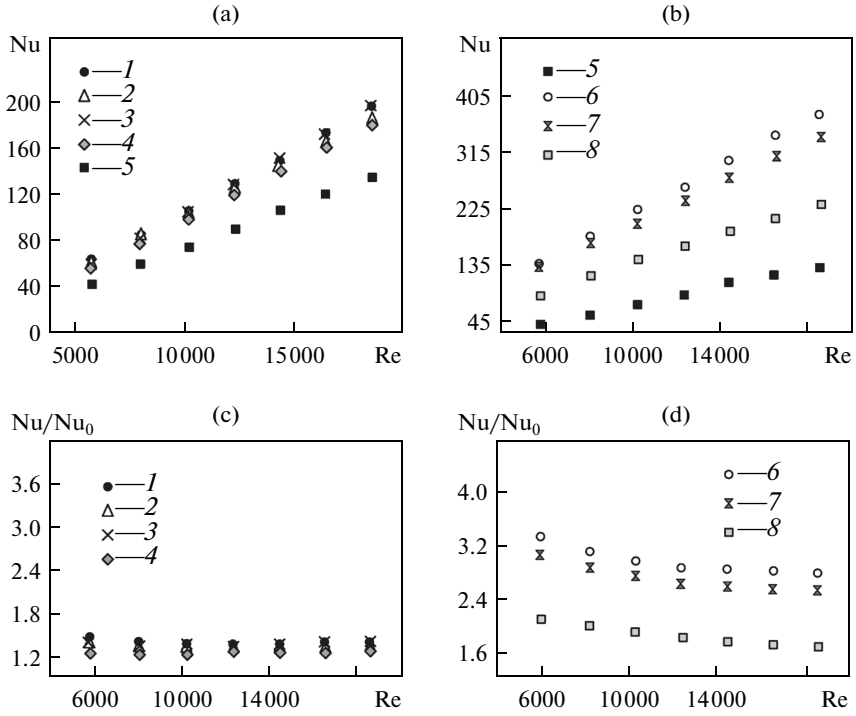

Fig. 6. The Nu (a, b) and Nu/Nu_0 (c, d) values at various Re numbers. Coiled wire inserts, *y*, mm: *1*—12; *2*—17; classic twisted tape, *y*, mm: *3*—30; *4*—45; *5*—plain tube; starry inserts, *y*, mm: *6*—0.58; *7*—0.50; *8*—0.31.

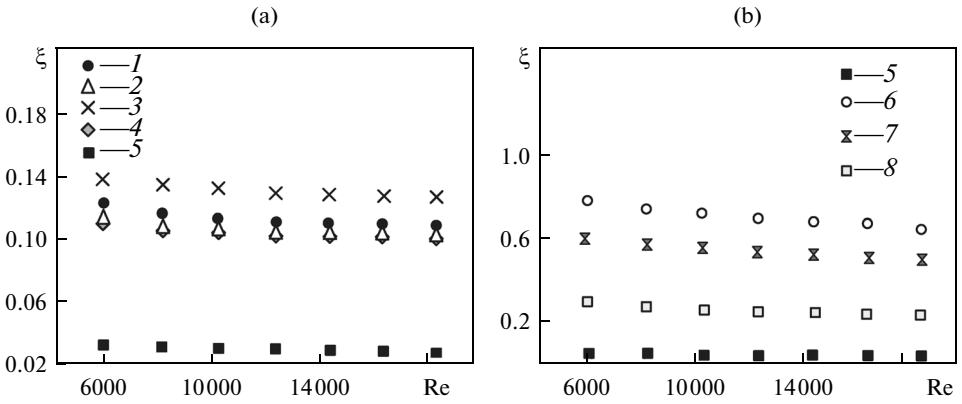

Fig. 7. The ξ values versus Re for tubes fitted with different inserts. The notation is the same as in Fig. 6.

Besides that the Nusselt number ratio for the case of starry insert is higher than those of the coiled wire inserts and classic twisted tape in the studied range of Reynolds numbers. For example, in the range of 5832 to 18518 Re numbers, the ratios of Nu/Nu_0 for the starry $A_{star}/A_{inlet} = 0.50$, coiled wire inserts ($y = 12$ mm) and classic twisted tape (y = 30 mm) are between 2.57–3.127, 1.433–1.543 and 1.389–1.474, respectively. The figure reveals that for the starry inserts, there are significant reductions of Nu/Nu_0 ratio values in lower Reynolds numbers and also the curve slope is decreased in higher values of Reynolds numbers. This confirms that it is more useful to use such inserts in lower Reynolds numbers.

In Fig. 7 the results of observed friction factor of different inserts are illustrated. The friction factors of plain tube and tube equipped with coiled wire inserts and classic twisted tape inserts in different pitch length (y) are depicted in Fig. 7a. Figure 7b shows the variation of friction factor with the Reynolds number values for various starry inserts. It is observed that the tube fitted with tube inserts shows a substantial increase in the friction factor (ξ) compared to the plain tube. As can be seen in Fig. 7a, friction factor increases with the decreasing of pitch length in both types of coiled wire inserts and classic twisted tape inserts the mean friction factors of the coiled wire inserts with pitch length 12 and 17 mm and classic twisted tape inserts with pitch length 30, 45 mm are 4.00, 3.69, 4.60 and 3.70 times the plain tube respectively.

It is seen that the mean friction factors of the starry are 24.9, 18.93 and 8.93 times the plain tube with surface ratios 0.58, 0.50, 0.31 respectively. In the process using tube inserts, the heat transfer enhancement can be obtained with the expense of increased pressure drop resulting from tube insertions. In order to determine the insertion performance, the parameter $TPF = (Nu/Nu_0)/(\xi/\xi_0)^{0.291}$ is used [30]. This parameter is called the Thermal Performance factor which means the comparison is made based on constant pumping power.

Figure 8 displays the variation of TPF value at different Reynolds numbers. This indicates that the role of inserts in increasing the turbulence intensity is more significant at lower velocities than at higher velocities. In addition, thermal performance factors are varied between 0.928 and 1.329 for the starry inserts, 0.922 and 1.036 for coiled wire inserts, and 0.89 and 0.935 for the classic inserts depending on the Reynolds number and surface ratios A_{star}/A_{inlet} or the pitch length (y). As can be seen in Fig. 8, thermal performance factors values of the starry inserts with A_{star}/A_{inlet} = 0.50 and 0.58 show small differences in the studied range of Reynolds.

The ratio of Nu/Nu_0, ξ/ξ_0 and thermal performance factor values for the starry inserts with various surface ratios, coiled wire inserts and classic twisted tape with various pitch length are compared in table.

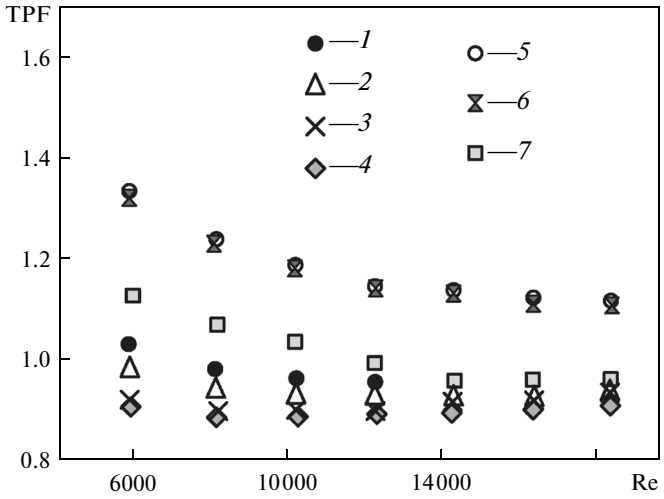

Fig. 8. Dependences of the TPF coefficient on the Re number for tubes with different types of inserts. Coiled wire inserts, y, mm: *1*—12; *2*—17; classic twisted tape, y, mm: *3*—30; *4*—45; starry inserts, y, mm: *5*—0.58; *6*—0.50; *7*—0.31.

Comparison between the characteristics of different types of inserts

Insert type	Nu/Nu_0	ξ/ξ_0	TPF
Starry insert:			
$A_{star}/A_{inlet} = 0.58$	3.015	24.900	1.183
$A_{star}/A_{inlet} = 0.50$	2.761	18.930	1.173
$A_{star}/A_{inlet} = 0.31$	1.909	8.930	1.010
Coiled wire insert:			
$y = 12$ mm	1.460	4.000	0.976
$y = 17$ mm	1.368	1.369	0.9355
Classic twisted tape:			
$y = 30$ mm	1.424	4.620	0.912
$y = 45$ mm	1.313	3.696	0.900

In comparison between, coiled wire inserts, classic twisted tape and starry inserts, it was found that there were higher performances by the starry inserts in terms of thermal performance factor.

CONCLUSIONS

(1) Starry inserts, coiled wire inserts and classic twisted tape tube inserts cause a remarkable increase in both pressure drop and heat transfer in comparison with the plain tube.

(2) The results show that the thermal performance factor is enhanced for all the used tube inserts except classic twisted tape.

(3) In the studied range of Reynolds number 5800–18500, the maximum thermal performance factor was obtained by the starry inserts with $A_{star}/A_{inlet} = 0.50$.

ACKNOWLEDGMENTS

This work was supported by the Yasouj Gas Company of Iran under the contract No. 89003.

REFERENCES

1. P. Parthasarathy, P. Talukdar, and V. R. Kishore, "Enhancement of heat transfer with porous/solid insert for laminar flow of a participating gas in a 3-D square duct," Numerical Heat Transfer; Part A: Applications **56** (9), 764–784 (2009).
2. S. Kiwan and M. S. Alzahrany, "Effect of using porous inserts on natural convection heat transfer between two concentric vertical cylinders," Numerical Heat Transfer; Part A: Applications **53** (8), 870–889 (2008).
3. N. Yucel and R. T. Guven, "Forced-convection cooling enhancement of heated elements in a parallel-plate channels using porous inserts," Numerical Heat Transfer; Part A: Applications **51** (3), 293 312 (2007).
4. X. Tong, J. A. Khan, and M. R. Amin, "Enhancement of heat transfer by inserting a metal matrix into a phase change material," Numerical Heat Transfer; Part A: Applications **30** (2), 125–141 (1996).
5. R. Sethumadhavan and M. R. Rao, "Turbulent flow heat transfer and fluid friction in helical wire coil inserted tubes," Int. J. Heat Mass Transfer **26** (12), 1833–1845 (1983).
6. K. Yakut and B. Sahin, "The effects of vortex characteristics on performance of coiled wire turbulators used for heat transfer augmentation," Appl. Therm. Eng. **24** (16), 2427–2438 (2004).
7. G. C. Kidd, Jr., "Heat transfer and pressure drop for nitrogen flowing in tube containing twisted-tapes," AIChE J. **15** (2), 581–585 (1969).
8. O. H. Klepper, "Heat transfer performance of short twisted-tapes," AIChE J. **35**, 1–24 (1972).
9. M. S. Lokanath, "Performance evaluation of full length and half length twisted-tape inserts on laminar flow heat transfer in tubes," in *Proceedings of the 14th National Heat and Mass Transfer Conference and Third ISHMT—ASME Joint Heat and Mass Transfer Conference*, IIT Kanpur, India, 1997, pp. 319–324.
10. A. Dewan, P. Mahanta, K. Sumithra Raju, and P. Suresh Kumar, "Review of passive heat transfer augmentation techniques," J. Power Energy **218**, 509–525 (2004).
11. S. Eiamsa-ard, C. Thianpong, and P. Promvonge, "Experimental investigation of heat transfer and flow friction in a circular tube fitted with regularly spaced twisted tape elements," Int. Commun. Heat Mass Transfer **33**, 1225–1233 (2006).
12. S. Jaisankar, T. K. Radhakrishnan, and K. N. Sheeba, "Experimental studies on heat transfer and friction factor characteristics of thermosyphon solar water heater system fitted with spacer at the trailing edge of twisted tapes," Appl. Therm. Eng. **29** (5–6), 1224–1231 (2009).
13. S. W. Chang, Y. J. Jan, and J. S. Liou, "Turbulent heat transfer and pressure drop in tube fitted with serrated twisted-tape," Int. J. Therm. Sci. **46** (5), 506–518 (2007).
14. S. W. Chang, T. L. Yang, and J. S. Liou, "Heat transfer and pressure drop in tube with broken twisted-tape insert," Exp. Therm. Fluid Sci. **32** (2), 489–501 (2007).
15. M. Rahimi, S. R. Shabanian, and A. A. Alsairafi, "Experimental and CFD studies on heat transfer and friction factor characteristics of a tube equipped with modified twisted tape inserts," Chem. Eng. Process. **48**, 762–770 (2009).
16. S. Al-Fahed, L. M. Chamra, and W. Chakroun, "Pressure drop and heat transfer comparison for both microfin tube and twisted-tape inserts in laminar flow," Exp. Therm. Fluid Sci. **18**, 323–333 (1998).
17. V. Zimparov, "Enhancement of heat transfer by a combination of a single-start spirally corrugated tubes with a twisted-tape," Exp. Therm. Fluid Sci. **25**, 535–546 (2002).
18. P. Bharadwaj, A. D. Khondge, and A. W. Date, "Heat transfer and pressure drop in a spirally grooved tube with twisted tape insert," Int. J. Heat Mass Transfer **52** (8), 1938–1944 (2009).

19. P. Sivashanmugam, P. K. Nagarajan, and S. Suresh, "Experimental studies on heat transfer and friction factor characteristics of turbulent flow through a circular tube fitted with right and left helical screw-tape inserts," Chem. Eng. Commun. **195** (8), 977–987 (2008).

20. R. X. Cai and C. H. Gou, "Discussion on the convective heat transfer and field synergy principle," Int. J. Heat Mass Transfer **50**, 5168–5176 (2007).

21. J. F. Guo, M. T. Xu, and L. Cheng, "The application of field synergy number in shelland- tube heat exchanger optimization design," Appl. Energy **86** (10), 2079–2087 (2009).

22. Q. Chen, J. X. Ren, and J. A. Meng, "Field synergy equation for turbulent heat transfer and its application," Int. J. Heat Mass Transfer **50**, 5334–5339 (2007).

23. E. Z. Ibrahim, "Augmentation of laminar flow and heat transfer in flat tubes by means of helical screw-tape inserts," Energy Conversion and Management **52**, 250–257 (2011).

24. T. S. Wang and Y. S. Chen, "Unified Navier–Stokes flow field and performance analysis of liquid rocket engines," AIAA Journal **9** (5), 678–685 (1993).

25. V. Gnielinski, "New equations for heat and mass transfer in turbulent pipe flow and channel flow," International Chemical Engineering **16**, 359–368 (1976).

26. F. W. Dittus and L. M. K. Boelter, *Calif. University of California Publications on Engineering* (Berkley, 1930).

27. L. F. Moody, "Friction factors for pipe flow," Trans. ASME **66**, 671–684 (1944).

28. B. S. Petukhov, "Heat transfer in turbulent pipe flow with variable physical properties," in *Advances in Heat Transfer*, Ed. by J. P. Harnett (Academic Press, New York, 1970), vol. 6.

29. S. Eiamsa-ard, P. Seemawute, and Kh. Wongcharee, "Influences of peripherally-cut twisted tape insert on heat transfer and thermal performance characteristics in laminar and turbulent tube flows," Experimental Thermal and Fluid Science **34**, 711–719 (2010).

30. H. Usui, K. Sano, K. Iwashhita, and A. Isozaki, "Enhancement of heat transfer by a combination of internally grooved tube and twisted tape," Int. Chem. Eng. **26** (1), 97–104 (1986).